Performance and discharge characteristics of doped β-MnO_2 in $ZnCl_2$ electrolytes

Buqui D. Desai*, Fernando S. Lobo and V.N. Kamat Dalal
Department of Chemistry, Goa University, P.O. Box, Bambolim 403 202, Goa (India)

(Received April 2, 1993; in revised form January 17, 1994; accepted January 21, 1994)

Abstract

The electrochemical performance of a number of doped MnO_2 samples was evaluated in the following electrolytes: (i) Leclanché; (ii) 25% $ZnCl_2$, and (iii) 25% $ZnCl_2$ with additives i.e., 2% LiCl and 1% NH_2SO_3H. Some of the molybdenum-doped MnO_2 samples perform well as cathode materials. The discharge duration appears to be better than that of the International Common Sample I.C-8 (chemical MnO_2) which was used as reference sample. Distinct improvement in the discharge duration is observed when both the additives are added simultaneously. Attempts were made to correlate the electrochemical reactivity of MnO_2 and the presence of cation vacancies, but no clear-cut conclusions could be drawn. The internal correlation of Ruetschi's parameters was satisfactory.

Introduction

It is well known that replacement of Leclanché cell electrolyte by an aqueous solution of $ZnCl_2$ has some advantages [1], especially with regard to leakage resistance and capacity. Heavy duty $ZnCl_2$ cells are already in the market. Very few published data are, however, available on the cell system using an aqueous solution of $ZnCl_2$ as electrolyte except those given in patents [2–4]. The overall reaction for this cell is given by the equation [5]:

$$8MnO_2 + 8H_2O + ZnCl_2 + 4Zn \longrightarrow 8MnOOH + ZnCl_2 \cdot 4Zn(OH)_2 \quad (1)$$

One of the factors limiting the capacity of the cathode in $ZnCl_2$ electrolyte seems to be the eventual drying out of the cell on continuous discharge [1]. Most of the patents [2–4] describe the use of an aqueous electrolyte containing 15 to 40 wt.% of $ZnCl_2$. This electrolyte is used in the manufacture of a cathode mix which contains 23 to 39 wt.% of H_2O, of a much higher level than is usually found in Leclanché mixes. The only recent report [6], which deals directly and extensively with the study of MnO_2 cathodes in $ZnCl_2$ electrolyte, has identified the solid phases and the composition of the residual electrolyte from chemical analyses and X-ray data. One other report [7], which gives the principal types of dry battery and their average characteristics, mentions that a typical commercial service capacity of a $ZnCl_2$ cell ranges from several hundred mAh to 9.0 Ah and the commercial energy density to be 88 Wh kg^{-1}. Tye [5] has observed that the $ZnCl_2$ Leclanché batteries can yield up to 100% more capacity than a normal Leclanché battery on continuous discharge, lasting less than a few days.

*Author to whom correspondence to be addressed.

SSDI 0378-7753(94)01912-F

Both the above-mentioned reports state that the nature of the discharge curve is sloping. In view of the fact that there is no report on the performance or the discharge behaviour of either β-MnO_2 or doped β-MnO_2 in $ZnCl_2$ electrolyte, it was decided to focus the attention on the study of these two aspects.

Experimental

Details of sample preparation, chemical composition, surface area, activity index and X-ray diffraction (XRD) data are presented in ref. 8, and given in Table 1. The cell assembly was based on the method reported in refs. 11 and 12. Three different electrolytes were used to study the discharge behaviour. These electrolytes were as follows:

(i) normal Leclanché, i.e., 5 M NH_4Cl + 2 M $ZnCl_2$, pH = 5–5.1;
(ii) 25% $ZnCl_2$, pH = 4.8, and
(iii) 25% $ZnCl_2$ + 2% LiCl + 1% NH_2SO_3H, pH = 4.9–5.0.

All the chemicals used were of Analar grade.

The discharge characteristics observed are presented in Table 2. The test cell was discharged continuously under fixed resistances of 100 and 40 Ω using 0.5 g of sample in 20 ml of 25% $ZnCl_2$ using a saturated calomel electrode (SCE) as reference electrode. The intermittent discharge at 84 Ω (4 h/day) was also carried out [13] and the data are presented in Table 3 and 4. The cell was also discharged at a constant current ('quasi-continuously') of 1 mA/0.1 g with SCE as reference electrode. In the 'quasi-continuous' discharge, the initial voltage of the cell (open-circuit voltage (OCV)) was first recorded and then the cell was discharged continuously for 5 h. The potential changes (close-circuit voltage (CCV)) were recorded manually at 30-min intervals on a digital multimeter. The cell was allowed to recuperate for 16 h to determine the OCV at 5 mAh discharge. The discharge was continued for 8 h/day and the cell was allowed to recuperate for 16 h. The cutoff voltage was 0 V versus SCE (approximately 1.0 V versus Zn). The energy density in Wh kg^{-1} was calculated from the usable energy in J g^{-1} which in turn was determined by integrating the area under the discharge curves (Table 2). The crystallite size [15] was calculated using full width at half maximum (FWHM) of (100) peak. The values are presented in Table 5.

Results and discussion

Chemical composition and formulae

Based on the chemical composition data (Table 1), the formulae were expressed in the format proposed by Brenet [17] which is as follows.

From the percentage of combined water, the number of neutral water molecules m in the crystal lattice was calculated using the relation:

$$m = \frac{91y + 2n\,(900 - y) - 3600}{18(100 - y)} \tag{2}$$

where, y is the percentage of the combined water in a sample; n is determined by the relation:

$$n = \frac{3 + x}{2} \tag{3}$$

TABLE 1

Chemical composition reactivity and formulae of manganese dioxides used in this work

Sample	Dopant (%)	MnO_2 (%)	Mn (%)	x in $MnO_{(1+x)}$	Combined H_2O (y) (%)	Surface area (ZIA) [9] ($m^2\ g^{-1}$)	Activity index [10]	$(MnO_2)_{(2n-3)}$	Formula $(MnOOH)_{(4-2n)} \cdot mH_2O$
S_0		98.43	63.18	0.9846	0.20	8.75	26.60	$(MnO_2)_{0.9846}$	$(MnOOH)_{0.0154} \cdot 0.002H_2O$
S_2	2.64(Mo)	81.48	64.55	0.7977	3.10	24.50	21.55	$(MnO_2)_{0.7976}$	$(MnOOH)_{0.2024} \cdot 0.051H_2O$
S_3	1.05(Mo)	93.48	61.80	0.9559	1.10	26.25	26.45	$(MnO_2)_{0.9558}$	$(MnOOH)_{0.0442} \cdot 0.031H_2O$
S_4	0.12(Mo)	95.40	65.92	0.9146	0.70	24.50	55.00	$(MnO_2)_{0.9146}$	$(MnOOH)_{0.0854}$
S_5	0.03(Mo)	96.70	64.02	0.9546	0.50	29.00	58.00	$(MnO_2)_{0.9546}$	$(MnOOH)_{0.0454} \cdot 0.001H_2O$
Ag-1	1.02(Ag)	87.10	56.31	0.9775	2.60	55.00	48.50	$(MnO_2)_{0.9774}$	$(MnOOH)_{0.0226} \cdot 0.118H_2O$
Ag-2	9.90(Ag)	88.84	54.94	1.0210	1.80	59.50	53.26	$(MnO_2)_{1.0210}$	$(MnOOH)_{0.0210} \cdot 0.099H_2O$
Li-1	0.03(Li)	99.65	62.14	1.0131	0.30	60.50	57.00	$(MnO_2)_{1.0130}$	$(MnOOH)_{0.0130} \cdot 0.021H_2O$
Li-2	0.06(Li)	97.94	63.18	0.9797	0.60	70.60	60.00	$(MnO_2)_{0.9593}$	$(MnOOH)_{0.0204} \cdot 0.019H_2O$
V	5.30(V)	82.02	59.06	0.8776	1.60	110.25	52.00	$(MnO_2)_{0.8776}$	$(MnOOH)_{0.1224} \cdot 0.031H_2O$
W	3.05(W)	94.04	60.43	0.9835	0.80	96.25	30.00	$(MnO_2)_{0.9834}$	$(MnOOH)_{0.0165} \cdot 0.016H_2O$
I.C-8		90.20	61.77	0.9229	2.42	79.52	60.91	$(MnO_2)_{0.9229}$	$(MnOOH)_{0.0771} \cdot 0.080H_2O$
I.C-4		88.75	59.88	0.9367	2.88	50.75	64.78	$(MnO_2)_{0.9367}$	$(MnOOH)_{0.0633} \cdot 0.1095H_2O$

TABLE 2

Discharge characteristics of MnO_2 in different electrolytes at 28 °C (room temperature)

5 M NH_4Cl + 2 M $ZnCl_2$				25% $ZnCl_2$			25% $ZnCl_2$ + 2% LiCl + 1% NH_2SO_3H		
Sample	Discharge duration (mAh)[a]	Usable energy (J g^{-1})	Energy density (Wh kg^{-1})	Discharge duration (mAh)[a]	Usable energy (J g^{-1})	Energy density (Wh kg^{-1})	Discharge duration (mAh)[a]	Usable energy (J g^{-1})	Energy density (Wh kg^{-1})
S_0	28	230	64	21	216	60	31	279	77
S_2	26	203	56	17	133	37	33	329	91
S_3	28	234	65	20	178	49	34	311	86
S_4	30	262	73	15	165	46	32	293	81
S_5	31	270	75	34	374	104	33	329	91
Li-1	29	225	62	24	228	63	28	237	66
Li-2	34	316	88	22	248	69	33	318	88
Ag-1	23	201	56	22	216	60	30	226	62
Ag-2	27	255	71	30	302	84	37	385	107
W	25	223	62	22	207	57	29	277	77
V	30	261	72	29	280	78	29	244	68
I.C-8				29	345	96	31	306	85

[a]For 0.1 g MnO_2, 1 mA constant current (discharge regime).

TABLE 3

Discharge characteristics of MnO_2 samples at 40 and 100 Ω continuous discharge

Sample	Ampere–hours	40 Ω continuous discharge in 25% $ZnCl_2$					100 Ω continuous discharge in 25% $ZnCl_2$				
	Theoretical Ah[a]	Ah expected[b]	Ah for 0.5 g sample[c]	Hours observed at cutoff voltage of 0 V vs. SCE	Ah observed	Utilization (%)	Ah expected	Ah for 0.5 g sample	Hours observed at cutoff voltage of 0 V vs. SCE	Ah observed	Utilization (%)
S_0	7.051	5.061	0.106	1.0	0.016	15	6.097	0.128	7.0	0.057	44
S_2	5.755	4.131	0.086	3.25	0.052	60	4.976	0.104	11.0	0.066	63
S_3	7.039	5.053	0.106	2.5	0.040	38	6.087	0.127	10.0	0.065	51
S_4	7.641	5.484	0.115	4.0	0.064	56	6.607	0.139	17.0	0.110	80
S_5	7.056	5.064	0.106	3.5	0.056	53	6.101	0.128	12.5	0.075	59
Li-1	7.398	5.310	0.111	4.0	0.064	58	6.397	0.134	6.5	0.052	38
Li-2	7.149	5.131	0.107	5.5	0.088	82	6.181	0.129	7.0	0.053	41
Ag-1	7.022	5.041	0.106	4.75	0.076	72	6.072	0.127	13.0	0.104	82
Ag-2	6.649	4.772	0.100	5.25	0.084	84	5.749	0.120	13.5	0.108	90
W	7.184	5.157	0.108	4.25	0.068	63	6.212	0.131	9.5	0.076	58
V	6.404	4.597	0.096	3.25	0.052	54	5.538	0.116	9.0	0.068	59
I.C-8	6.654	4.776	0.100	6.0	0.096	95	5.754	0.121	15.0	0.127	105

[a]Theoretical Ah were calculated using Ruetschi's values of C_w Ah g^{-1} and in samples S_4, Ag-2 and Li-1, Atlung's values of Ah g^{-1} were used in the calculations.

[b]The expected Ah for a given resistance regime were calculated using the formulae proposed by Huber [14].

[c]Ah for 0.5 g for different regimes were calculated by dividing the product of expected Ah and 0.5 g by 23.7825 g is the amount of MnO_2 taken in a dry mix in a 'D'-size Leclanché cell [9].

TABLE 4

Discharge characteristics of MnO_2 samples in 25% $ZnCl_2$ (intermittent discharge)

Sample	Ampere–hours	84 Ω intermittent discharge 4 h/day using 25% $ZnCl_2$ at 28 °C				
	Ah theoretical	Ah expected	Ah for 0.5 g sample	Hours observed at cutoff voltage of 1.0 V vs. Zn	Ah observed	Utilization (%)
S_0	7.051	5.231	0.109	9.0	0.090	83
S_2	5.755	4.269	0.089	16.0	0.160	178
S_3	7.039	5.222	0.109	16.0	0.176	160
S_4	7.641	5.669	0.119	16.0	0.160	134
S_5	7.056	5.234	0.110	13.0	0.130	118
Li-1	7.396	5.489	0.115	10.0	0.100	87
Li-2	7.149	5.303	0.111	10.0	0.112	100
Ag-1	7.022	5.210	0.109	12.0	0.120	110
Ag-2	6.649	4.932	0.103	11.0	0.132	128
W	7.184	5.330	0.112	14.0	0.126	113
V	6.404	4.751	0.099	10.0	0.120	120
I.C-8	6.654	4.937	0.103	12.0	0.120	116

TABLE 5

Correlation of efficiency of MnO_2 samples in different electrolytes, vacancy fraction and crystallite size

Sample	Vacancy fraction ($\times 10^{-3}$)	Crystallite size Å (h k l (100) peak)	25% $ZnCl_2$ as electrolyte		Efficiency (Leclanché)	Efficiency (Additives)
			Energy density (Wh Kg^{-1})	Efficiency[a]		
S_0	0.98	277	60	70	94	104
S_2	24.64	274	37	91	139	176
S_3	15.49	120	49	73	102	124
S_4		410	46	56	113	120
S_5	0.74	205	104	102	106	102
Li-1		205	63	77	93	90
Li-2	10.00	274	69	74	115	112
Ag-1	55.48	246	60	84	88	114
Ag-2	47.20	336	84	107	97	132
W	15.00	169	57	77	88	102
V	8.18	274	78	133	138	133
I.C-8	38.72		96	114	177	122

[a]Efficiency calculations are based on theoretical mAh g^{-1} which in turn were calculated from Atlung [16].

where, x in MnO_{1+x} is the ratio of reducible Mn to the total Mn and is calculated using the relation:

$$x = \frac{0.632 \times \%\ MnO_2}{\%\ Mn} \tag{4}$$

Simultaneously from the m values of Brenet, the cation vacancy fraction 'x' which represents the Mn vacancies according to Ruetschi [18] (see Table 6) was calculated.

The proposed cation vacancy model leads to the following formula for manganese dioxide:

$$Mn_{(1-x-y)}^{4+} \cdot Mn_y^{3+} O_{(2-4x-y)}^{2-} \cdot OH_{(4x+y)}^{-} \tag{5}$$

The parameters 'x' (fraction of vacancies) and y (fraction of Mn^{3+} ions in the above-mentioned equation are related to the parameters 'n' and 'm'. The relation between Brenet's formula and that of Ruetschi is as follows:

$$'x' = \frac{m}{2+m} \tag{6}$$

$$y = \frac{4\,(2-n)}{2+m} \tag{7}$$

and

$$n = \frac{4\,(1-x)-y}{2\,(1-x)} \tag{8}$$

$$m = \frac{2x}{1-x} \tag{9}$$

The vacancy fraction values vary from 0.055 in the case of Ag-1 sample to 0.0009 in the case of pure β-MnO_2 (S_0). Consequently, the y value of Ruetschi which represents Mn^{3+} in MnO_2 is found to vary between 0.121 in the case of V–MnO_2 to 0.015 in S_0, and in at least three cases, i.e., S_4, Li-1, and Ag-2, the y values are found to be negative indicating complete absence of Mn^{+3} in the MnO_2 lattice. The percentage of structural water as predicted by Ruetschi [18] is also uniformly low, i.e., of the order of 10^{-3}. It varies from 0.023 to 0.0003% when $y=0$. According to Ruetschi it is the vacancy fraction 'x' which is responsible for 'electrochemical activity' and not so much the structure *per se*. In an earlier publication [19] we confirmed this in the case of γ-MnO_2. But in this case it is difficult to arrive at a categorical conclusion as the observed electrochemical capacity does not have a direct correlation with the vacancy fraction. According to Ruetschi the lower the vacancy fraction the higher is the % C_w, i.e., theoretical electrochemical capacity. If this criterion is applied, a few discrepancies are observed in the case of MnO_2 investigated here. For instance, S_5 (containing the least amount of molybdenum) and the smallest values of vacancy fraction 'x' and structural water, has a % C_w of 96 where C_w [18] is the theoretical (maximum) electrochemical capacity deliverable per unit weight. On the other hand Li-2, having a higher value of 'x' and % H_2O, has 98% C_w. Moreover, the observed capacity in mAh (see Table 2) is higher in the case of S_5 than in the case of Ag-2 in both the electrolytes, Leclanché as well as pure $ZnCl_2$. As far as the energy density and efficiency are concerned, there seems to be a linear relationship between these two parameters and the vacancy fraction 'x' in $ZnCl_2$ electrolyte (Fig. 1). In the case of pure $ZnCl_2$, however, the energy density shows a rather peculiar trend. It increases as the vacancy fraction decreases. This behaviour, however, cannot be easily explained. Among the remaining materials there is a considerable scatter of the values. Both the Ag-doped samples do not conform to the pattern. In the case of molybdenum-doped family the % MnO_2 increases as the molybdenum content decreases. This is in conformity with the results reported by Valand [20]. The activity indices of S_4 and

TABLE 6

Correlation of physical and electrochemical properties of MnO_2 samples prepared in this work

Sample	m	x ($\times 10^{-3}$) (Ruetschi)	y (Ruetschi)	Mol. wt. (g)	$\%H_2O$ $y=0$ (Ruetschi)	C_w[a] (%)	C_v (%)	V $(nm)^3$	Density (g cm^{-3}) $y=0$	Pycnometric density (g cm^{-3})
S_0	0.002	0.98	0.015	88.88	0.0004	96.0	96.0	5.50	5.25	4.31
S_2	0.050	24.64	0.202	85.59	0.010	79.0	77.0	5.53	5.14	4.41
S_3	0.031	15.49	0.043	85.19	0.006	96.0	96.0	5.47	5.23	4.21
S_4								5.56		4.39
S_5	0.001	0.74	0.045	86.15	0.0003	96.0	96.0	5.12	5.24	4.17
Li-1	0.021	10.41						5.58	5.14	4.32
Li-2	0.019	10.00	0.020	86.44	0.004	98.0	96.0	5.55	5.17	4.40
Ag-1	0.117	55.48	0.021	83.77	0.024	96.0	92.0	5.57	5.01	3.96
Ag-2	0.099	47.20	0.000	84.52	0.020	98.0	95.0	5.51	5.09	4.31
W	0.031	15.00	0.016	85.91	0.006	98.0	98.0	5.48	5.22	4.16
V	0.016	8.18	0.121	86.63	0.003	87.0	84.0	5.67	5.07	4.22
I.C-8	0.081	38.72	0.074	84.97	1.642	98.44	102.45	0.111	5.09	4.67
I.C-4	0.109	51.91	0.060	84.30	2.218	97.85	101.06	0.111	5.05	4.52

[a]Theoretical electrochemical capacity calculated on the basis of Atlung [16] agree well with the ones calculated from Ruetschi formula [18].

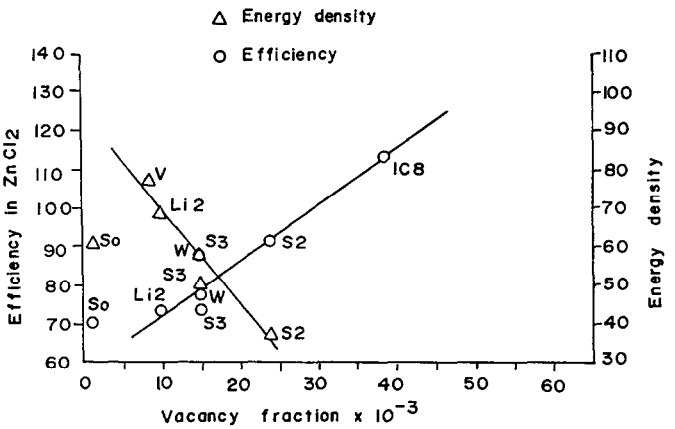

Fig. 1. Relation between efficiency, energy density and vacancy fraction under the discharge regime of 1.0 mA 0.1 g^{-1} of MnO_2.

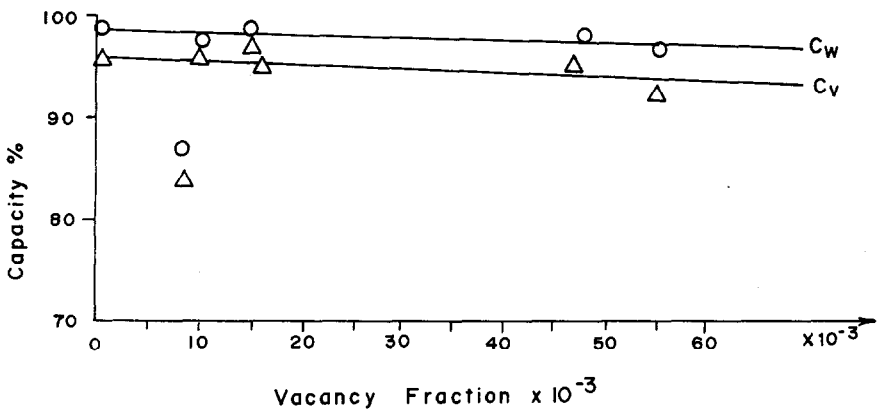

Fig. 2. Theoretical electrochemical capacity per unit weight (Ah g^{-1}) and per unit volume (Ah cm^{-3}) as a function of Mn^{4+} vacancy fraction 'x'.

S_5 also show a considerable increase but the specific surface area increases only marginally with respect to S_0 (the undoped sample). On the other hand, both specific surface and the activity index show an appreciable increase in the case of all other doped samples. The choice of the dopants was determined by their ionic radii. The ionic radii of the dopants range between 0.54 and 0.62 Å, or thereabouts, except in the case of Ag^{+}; 0.62 Å is the ionic radius of Mn^{+3} and 0.54 Å that of Mn^{4+}. The purpose was to achieve substitutional replacement of either Mn^{4+} or Mn^{3+} in the host MnO_2 lattice by the dopant. As far as the internal correlation of Ruetschi's parameters is concerned, it is satisfactory (Fig. 2) in as much as most of the samples show a linear relationship when the vacancy fraction is plotted against % C_w, except S_2 and V–MnO_2.

It is worth mentioning that there seems to be a sufficiently good agreement in the case of S_0, S_3, S_5, Li-2, and W samples between the theoretical Ah capacity obtained from the Atlung's model [16] with those from Ruetschi [18] (see Table 7).

TABLE 7

Theoretical electrochemical capacity C_w

Sample	Ah g^{-1} (Ruetschi) [18]	Ah g^{-1} (Atlung) [16]
S_0	0.297	0.298
S_2	0.242	0.187
S_3	0.296	0.275
S_4		0.321
S_5	0.297	0.284
Li-1		0.311
Li-2	0.301	0.296
Ag-1	0.295	0.262
Ag-2		0.280
V	0.269	0.218
W	0.302	0.294
I.C-8	0.280	0.254

Ruetschi's method

The theoretical (maximum) electrochemical capacity deliverable per unit weight (C_w), or unit volume (C_v), calculated using the relation given by Ruetschi [18] is as follows:

$$C_w = \frac{(1-x-y)26.80}{\text{mol. wt.}} \text{ (Ah g}^{-1}\text{)} \tag{10}$$

where, the parameters 'x' (fraction of vacancies) and y (fraction of Mn^{3+} ions) in eqn. (5) are related to the parameters x and m by the eqns. (6)–(9).

Structure

Almost all the samples prepared in this work have a β-MnO_2 structure as no additional lines are seen in any of the XRD patterns, except for some traces of γ-Mn_2O_3. Even the Ag-2 sample which contains 9.9% of Ag does not exhibit any new lines. Also in the case of S_3, Ag-1, Ag-2, and V samples the (100) intensity line shifts to higher angles. The crystallite size, however, shows some variations with respect to the undoped sample S_0, except S_3 and S_4 which show large variations from S_0 (277 Å) (Table 5). Since a large amount of silver was incorporated without the appearance of a second phase, a solid solution of silver with MnO_2 was expected. But there was no evidence for this in the lattice parameters. The available oxygen content however, is much less (88.84%) in Ag-2 compared with the other samples. Li-2 sample, on the other hand, does exhibit some minor changes in its XRD pattern (Fig. 3). In general, there is a broadening of lines which is reflected in the crystallite size getting reduced in the case of V–MnO_2, S_3, S_5, Li-1 and Ag-1. In the case of the remaining samples it either remains the same as that of S_0 or shows a slight increase. XRD density values also agree well with reported literature values [18]. The discrepancy between the pycnometric density and XRD density is similar to that observed in γ-MnO_2 samples [21]. The tap density, however, is uniformly higher than that of γ-MnO_2. An investigation in the surface of these doped samples with the help of electron spectroscopy

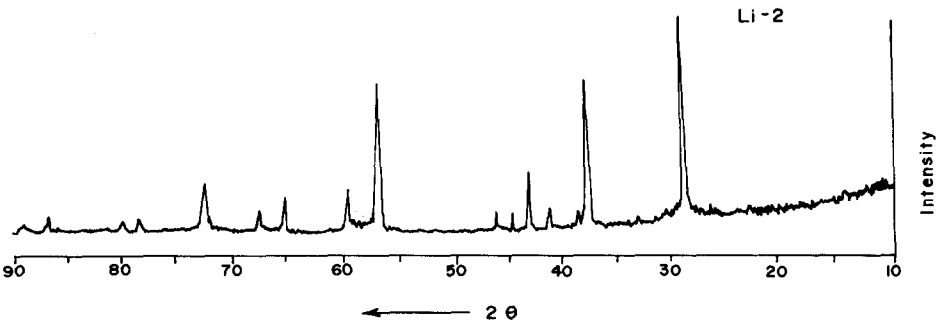

Fig. 3. X-ray diffractogram of Li-2 sample.

for chemical analysis (ESCA) will be communicated elsewhere [22]. These studies clearly reveal the presence of dopants on the surface in almost all cases, exceptions being S_4 and S_5 which contain very small amounts of molybdenum.

Electrochemical evaluation

It is evident from the data presented in Table 2 that the performance in terms of mAh capacity is rather uneven. It is only the Ag-2 sample which shows a distinct improvement from Leclanché electrolyte to pure $ZnCl_2$, and $ZnCl_2$ with additives. The energy density on the other hand improves considerably. The reported energy density of 88 Wh kg^{-1} [7] is exceeded by S_2, S_5, Li-2 and Ag-2 samples prepared in this work. The international common standard sample I.C-8, however, performs well when the discharge is carried out at a constant current of 1 mA. In other discharge regimes, i.e., 40 and 100 Ω continuous discharge and in 84 Ω intermittent discharge doped β-MnO_2 perform better than I.C-8. In general, one might say that some doped MnO_2s prepared here exhibit a better consistency when different discharge regimes are used. For instance, both in the case of constant current, in the case of continuous tests on 40 and 100 Ω, and in intermittent test of 84 Ω the performances of S_2, S_5, Li-2 and Ag-2 are more or less uniform. In the presence of additives, however, the energy density of I.C-8 decreases substantially. The decrease is all the more pronounced as compared with the Leclanché electrolyte. The general improvement in the discharge characteristics of doped MnO_2 in the presence of additives may probably be due to either one or all of the following factors acting in conjunction with one another:

(i) increased conductivity of the electrolyte due to the addition of LiCl;

(ii) presence of NH_2^+ ions in conjunction with LiCl, and

(iii) corrosion inhibiting influence of sulfamic acid.

The transport number t_m of LiCl ions can contribute to the current-carrying capacity and thus help in the discharge.

Ag-2 shows a substantial improvement both in terms of mAh capacity obtained, i.e., from 30 to 37 per 0.1 g and in terms of the energy density, i.e., from 84 to 107 Wh kg^{-1}. This may be due to the presence of silver itself which must be enhancing the conductivity of the cathode mix to a considerable degree. The energy density of V–MnO_2, however, shows a slight decrease in the presence of additives. The efficiency of all the samples in general shows an improvement in the presence of additives. The I.C-8 sample, on the other hand, shows a decrease in efficiency both in pure $ZnCl_2$, and $ZnCl_2$ with additives, as compared with its efficiency in Leclanché electrolyte (Table 5). The crystallite size does not seem to have a direct correlation with the theoretical electrochemical capacity. The vacancy fraction, however, does show a linear

relationship with both the energy density and the efficiency (in the presence of additives as well). Due allowance should be made for the fact that the observed Ah capacity computed in this work was calculated from the average of the current recorded when the discharge was carried out continuously through a fixed resistance. The results of the quasi-continuous discharge are plotted in Figs. 4 to 9. The flattish nature of the potential versus mAh capacity plots in case of β-doped samples, as well as I.C-8, is rather unusual and has not been reported thus far. All the earlier workers, who have done extensive studies on the mechanism of the electrochemical reduction of MnO_2 [19, 23, 24], have agreed upon the single-phase homogeneous reduction of MnO_2 and hence on the sloping potential-reduction curve. Even those who have been working on the pure $ZnCl_2$ electrolyte reported that the discharge curves are sloping [6]. But the cathode mix invariably contains γ-MnO_2. The flat nature from approximately 0.3 V versus SCE (approximately 1.21 V versus Zn) obtained in this work, under 1.0 mA constant current, turns into a normal sloping one when the discharge is carried out at higher current drains or at a smaller fixed resistance. This means that it is either not a true two-phase reduction, or it is a two-phase reduction only under very mild electrochemical reduction conditions. In any case, what is of relevance to the battery technologist is the fact that the potential remains constant for about 26 h at a discharge drain of 1 mA g^{-1}. The service obtained on continuous discharge in any one of the electrolytes used, whether at constant current or constant resistance, is not substantially higher than in the classical Leclanché system. The marginal improvement is exhibited by Ag-2, S_5 and Li-2 under certain specified discharge regimes but there is no large increase of capacity as indicated by Tye [5]. It needs to be emphasized, however, that the present results are obtained on a test cell and, therefore, caution must be exercised in extrapolating these data to commercial $ZnCl_2$ batteries.

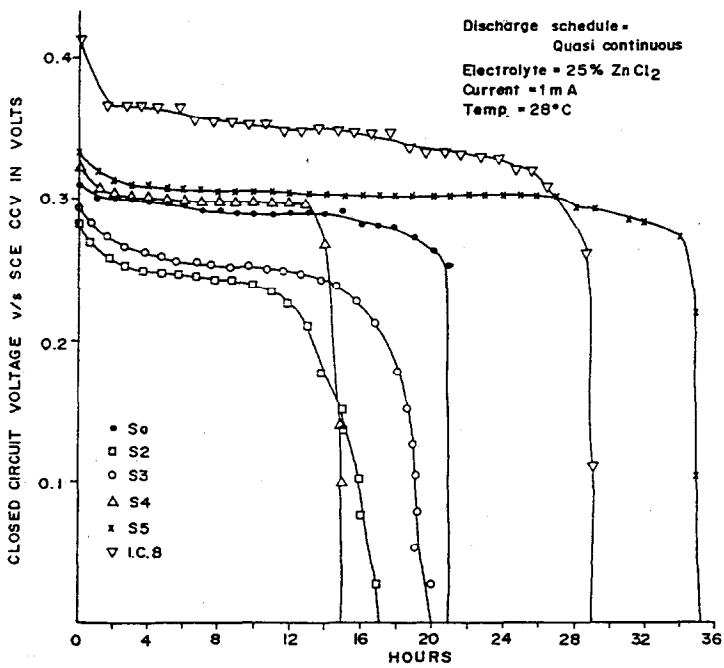

Fig. 4. Discharge curves at constant current.

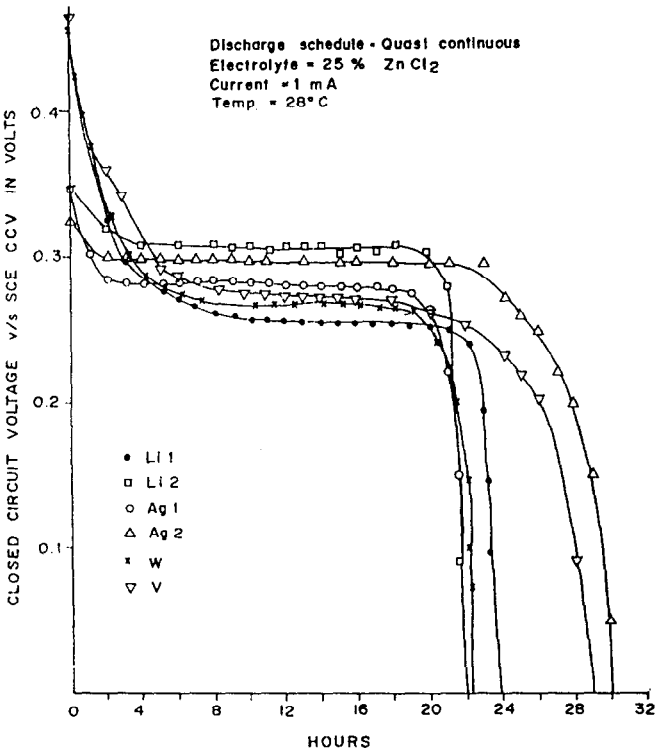

Fig. 5. Discharge curves at constant current.

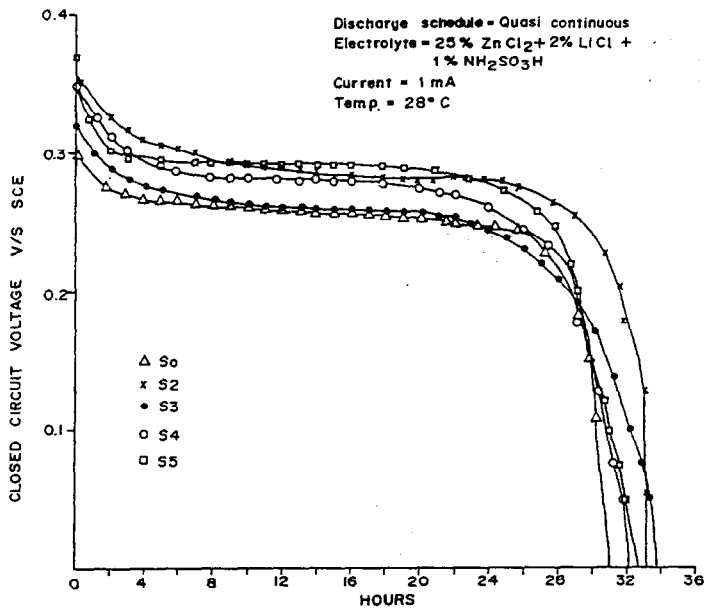

Fig. 6. Discharge curves at constant current.

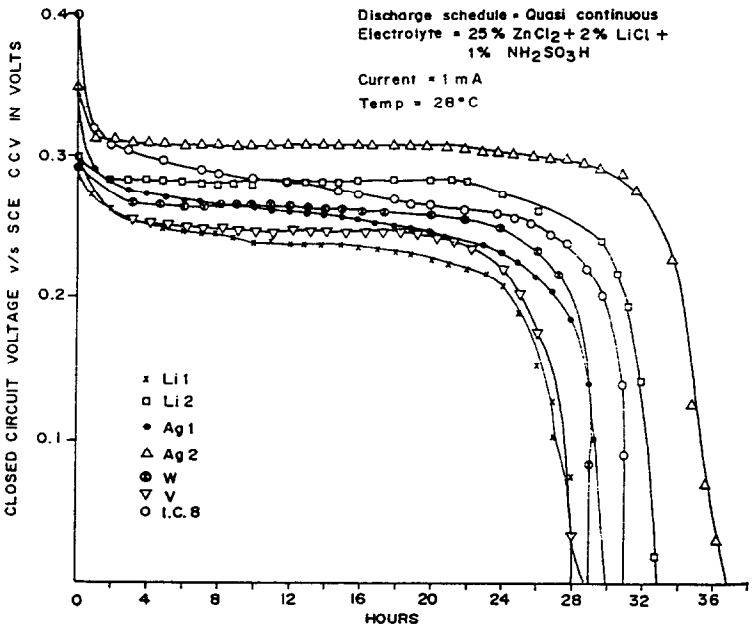

Fig. 7. Discharge curves at constant current.

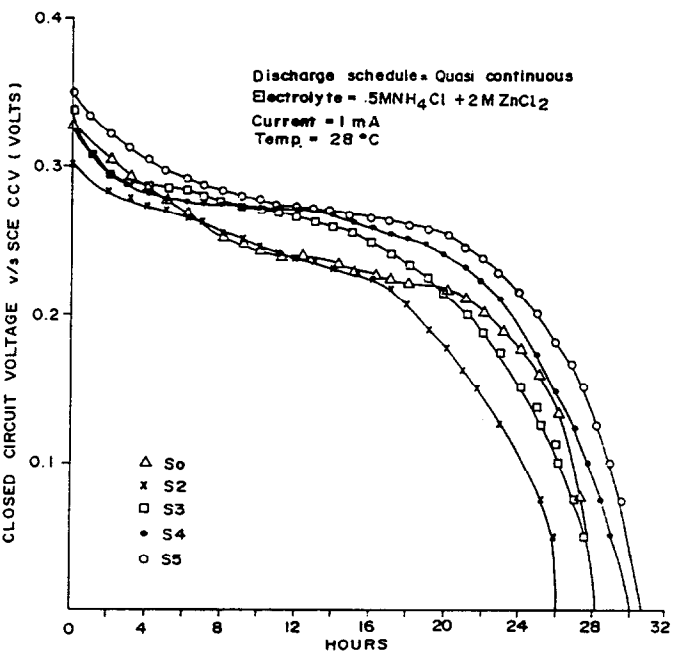

Fig. 8. Discharge curves at constant current.

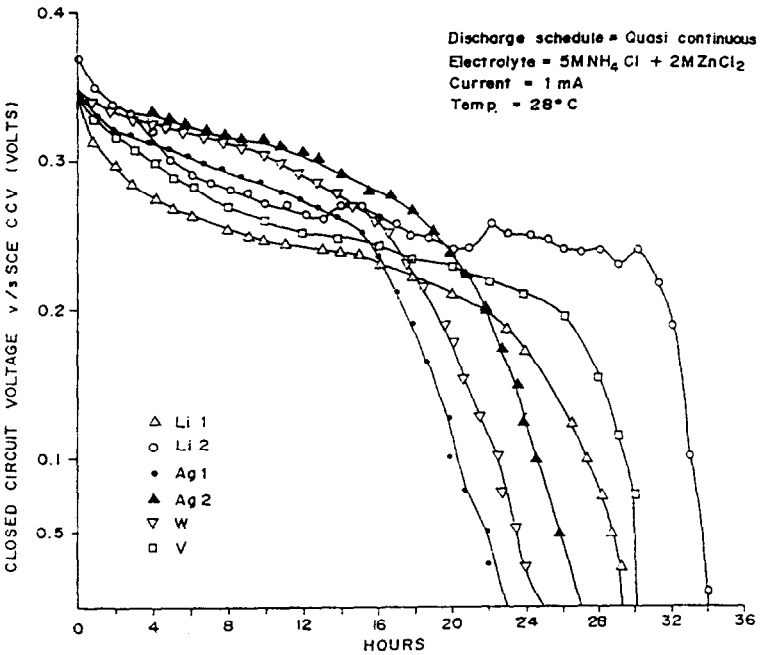

Fig. 9. Discharge curves at constant current.

Capacity variation with discharge rate: continuous discharge through a fixed resistance of 40 and 100 Ω

In 25% $ZnCl_2$

The variation of voltage versus hours of service obtained are depicted in Figs. 10 to 12. It is evident from these Figures that Ag-2 compares rather favourably with the reference sample I.C-8. Similar is the case with S_5 (molybdenum-doped sample with the least amount of molybdenum). Curiously enough, Li-2 appears to yield a better service under a 40 Ω constant resistance test than the 100 Ω test. At this stage of the discussion it is not possible to propose a tenable explanation for this behaviour of Li-2 which gives a comparable if not better performance than I.C-8 under different discharge regimes (see Table 3). The initial CCV varies between 0.28 to 0.36 V versus SCE which is approximately 1.18 to 1.24 V versus Zn. The nature of the voltage versus the discharge duration in hours is distinctly sloping and not flattish as in the case under constant-current discharge.

Intermittent discharge at 84 Ω (4 h/day) [13]

In this test, Zn was used both as counter and reference electrodes. The expected Ah were computed by adaptation of the formula proposed by Huber for Leclanché cells [14]:

$$Ah_{expected} = Ah_{theoretical}\,[1 - \exp(-K^{I}\,(R/C)^{1/2}) - \exp(-K^{II}\,(1/C)^{-1/2})(R/C)^{-n}] \qquad (11)$$

where, $n = 0.2$, $K^{I} = 0.2$, $K^{II} = 12$, R is the discharge resistance, and $C = \text{h/day}/24 = 4/24 = 0.1666$.

The observed Ah capacity was obtained by multiplying the average of the current recorded from time to time till the end of discharge at 1.0 V cutoff versus Zn by

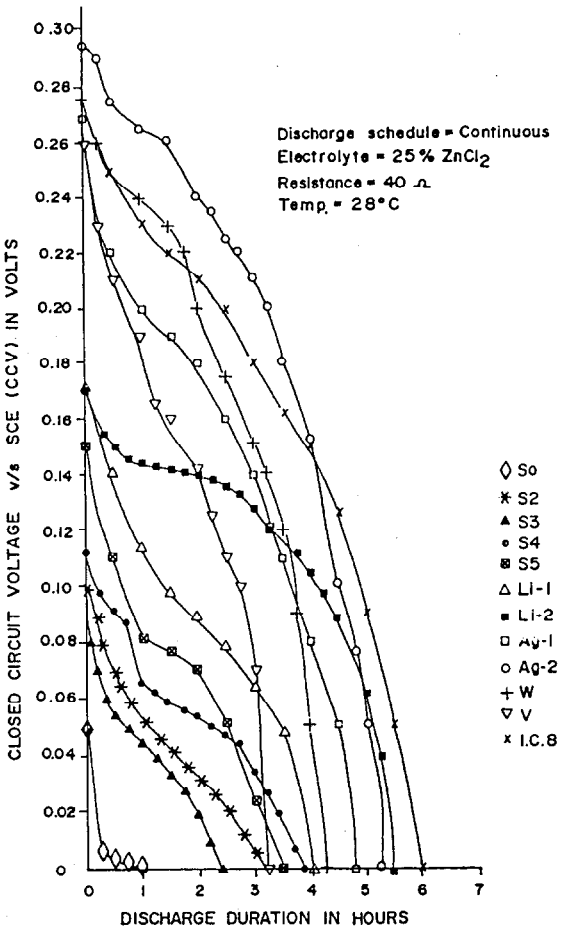

Fig. 10. Discharge curves at constant resistance.

time. The percentage utilization was thus obtained by assuming the expected Ah to be 100%.

The initial CCV remains at, or a little below, 1.2 V versus Zn, for all the samples. The total service obtained in the case of doped samples compares favourably with I.C-8. The molybdenum-doped samples seem to perform much better than the I.C-8 sample as is evident from the hours of service, i.e., 16 (intermittent discharge) in the case of all molybdenum-doped samples, except S_5, against the 12 of I.C-8 (see Table 4). Inspite of the fact that Ag-2, Li-2, S_5 and V show a great deal of promise under different discharge regimes, they do not exhibit a consistent pattern in terms of the service obtained. This rather erratic behaviour is more pronounced in the case of Li-2, S_5, S_2 and Ag-1. For example the percentage utilization of Li-2 is 82 under 40 Ω and 41 under 100 Ω discharge. I.C-8, on the other hand, shows a high percentage utilization under all the three tests and hence a consistent pattern.

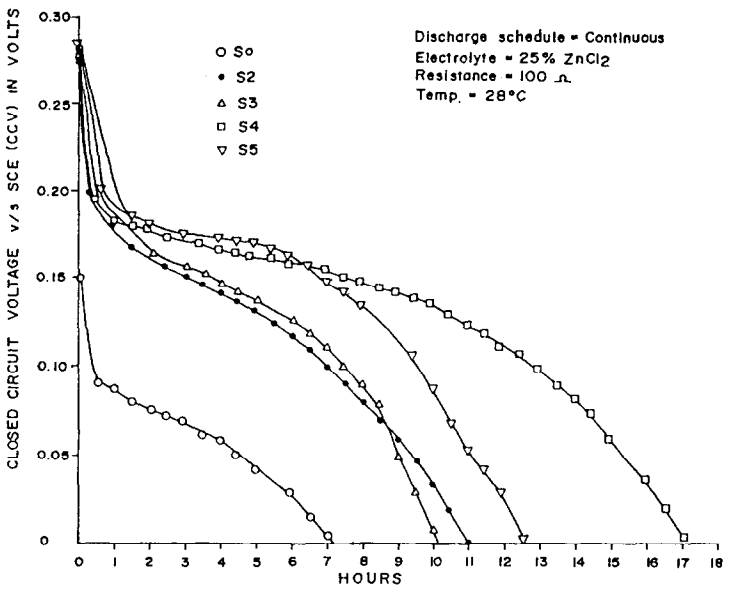

Fig. 11. Discharge curves at constant resistance.

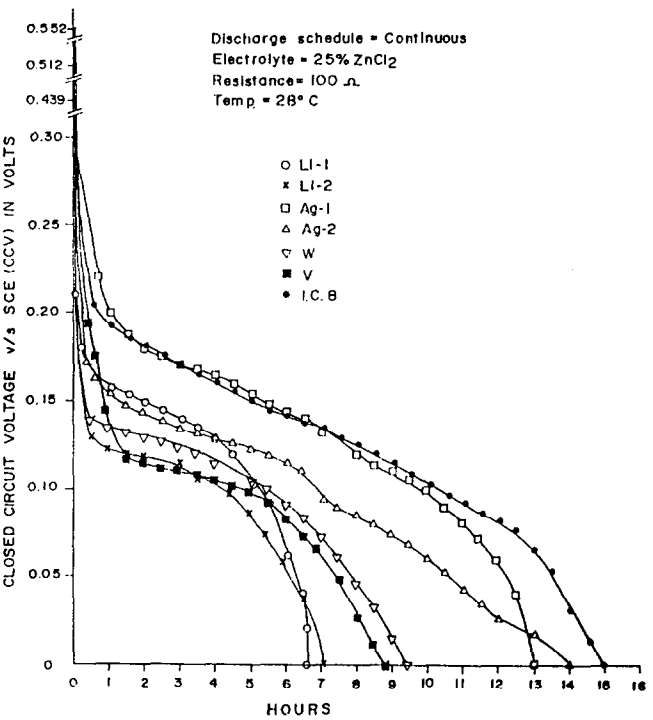

Fig. 12. Discharge curves at constant resistance.

Conclusions

Some of the molybdenum-doped samples along with lithium and silver-doped MnO_2 seem to perform very well in $ZnCl_2$ electrolytes. The discharge duration appears to be better than that of I.C-8 which was used as reference sample. In general, Li–MnO_2, Ag–MnO_2 and Mo–MnO_2 (S_5 sample) seem to be the most promising cathode materials amongst the tested MnO_2. Distinct improvement in the discharge duration as well as in energy density is observed when LiCl and NH_2SO_3H are added together to the $ZnCl_2$ solutions. The discharge curves are flat when the discharge is carried out at 1 mA 0.1 g^{-1}. The discharge behaviour of Ag-2 is the best in $ZnCl_2$ with additives, intermediate in pure $ZnCl_2$, and the least in classical Leclanché electrolyte. The energy density improves considerably in most of the samples in the presence of additives. The performance of S_2, S_5, Li-2 and Ag-2 are noteworthy. The energy density of the above-mentioned samples exceeds the reported value of 88 Wh kg^{-1}. In the presence of additives, however, the energy density of the I.C-8 sample decreases substantially. The flattish nature of the potential versus mAh capacity plots in the case of all samples under low current drain is rather unusual. The discharge seems to proceed via a pseudo two-phase reduction as against a single-phase reduction in classical Leclanché and/or alkaline KOH systems. There seems to be a good agreement in the case of S_0, S_3, S_5, Li-2, and W between the theoretical Ah obtained from Atlung's model with those obtained from Ruetschi's model. The silver-doped samples are the best as far as the correlation of vacancy fraction *'x'* with efficiency and energy density is concerned. The Ag-2 and I.C.-8 samples show a good performance in all three regimes at constant current of 1 mA and in fixed resistance 40 and 100 Ω continuous discharge. S_5 gives 34 mAh in 25% $ZnCl_2$ but relatively poor performance in 40 Ω continuous discharge regime. The percentage utilization of Ag-2 sample is highest in both the discharge regimes, i.e., 84% under 40 Ω discharge and 90% under 100 Ω discharge. Ag-1 also shows a consistent behaviour in both the discharge regimes.

References

1 N.C. Cahoon, in N.C. Cahoon and G.W. Heise (eds.), *The Primary Battery*, Vol. 2, Wiley, 1976, p. 138.
2 W. Krey, *Ger. Patent No. 2 021 285* (Nov. 11, 1971); *Ger. Patent No. 2 021 286* (Nov. 18, 1971).
3 W. Krey, *US Patent No. 3 358 364* (Jan. 26, 1971).
4 VARTA–Pertrix–Union Gesellschaft, *Indian Patent No. 112 711* (Dec. 16, 1968); *US Patent No. 3 558 364* (Jan. 26, 1971).
5 F.L. Tye, in M. Barak (ed.), *Primary Batteries for Civilian Use, Electrochemical Power Sources*, Peter Peregrinus, London, 1980, p. 120.
6 B. Poussard, V. Dechenaux, P. Croissant and A. Hardy, in J. Thompson (ed.), *Power Sources 7*, Academic Press, London, 1979, pp. 445–461.
7 T.R. Crompton, *Primary Cells, Small Batteries*, Vol. 2, Wiley, New York, 1983, p. 3.
8 B.D. Desai, F.S. Lobo and V.N. Kamat Dalal, *J. Power Sources,* to be published.
9 A. Kozawa, in K.V. Kordesch (ed.), *Batteries, Manganese Dioxide*, Vol. 1, Marcel Dekker, New York, 1974, p. 497.
10 K. Takahashi, *Electrochim. Acta, 26* (1981) 1467.
11 J.B. Fernandes, B.D. Desai and V.N. Kamat Dalal, *Electrochim. Acta, 29* (1984) 181.
12 A. Kozawa, *Prog. Batteries Solar Cells, 2* (1979) 106.
13 *American National Standard* (ANS) *C18.1*, 1972.
14 R. Huber, in K.V. Kordesch (ed.), *Batteries, Manganese Dioxide*, Vol. 1, Marcel Dekker, New York, 1974, pp. 137, 144.

15 L.V. Azaroff and M.J. Buerger, *The Powder Method in X-ray Crystallography*, Mc-Graw Hill, New York, 1958, p. 254.
16 S. Atlung and T. Jacobsen, *Electrochim. Acta, 26* (1981) 1455.
17 J.P. Brenet, M. Cyrankowska, G. Ritzler, R. Saka and K. Traore, *Proc. MnO_2 Symp. Cleveland, OH, USA*, Vol. 1, 1975, p. 274.
18 P. Ruetschi, *J. Electrochem. Soc., 131* (1984) 2738.
19 B.D. Desai, R.A.S. Dhume and V.N. Kamat Dalal, *J. Appl. Electrochem., 18* (1988) 71.
20 T. Valand, *J. Power Sources, 1* (1976/77) 71.
21 B.D. Desai, R.A.S. Dhume and V.N. Kamat Dalal, *J. Appl. Electrochem., 18* (1988) 64.
22 F.S. Lobo, V.N. Kamat Dalal and B.D. Desai, communicated elsewhere.
23 R. Huber and J. Bauer, *Electrochem. Technol., 5* (1967) 542.
24 A. Kozawa, in J. Thompson (ed.), *Power Sources 7*, Academic Press, London, 1979, pp. 485–500.